



Three is enough: Optimization of regions of interest selection for accurate estimation of proton density fat fraction in liver from magnetic resonance images

F. ROCHE¹, F. VINCENT¹, J. MARY¹, S. ZABBATINO², S. HOLLAND²

¹ Medpace, Lyon, France

² Medpace, Cincinnati, Ohio, United States



1 INTRODUCTION

Proton Density Fat Fraction (PDFF) measured by Magnetic Resonance Images (MRI) is now widely accepted as a biomarker for liver fat fraction in non-alcoholic fatty liver disease (NAFLD) and steato-hepatitis (NASH), correlating highly with both MR spectroscopy and histology of liver biopsies¹.

2 AIM

- Demonstrate that average PDFF (aPDFF) from 3 spatially well distributed Regions Of Interest (ROIs) correlates highly with aPDFF from 9 ROIs placed in each of the 9 Couinaud segments² (S) in the liver.
- Obviate more complicated, time-consuming and artifact-prone ROI strategy for liver fat measures.

3 METHOD

- PDFF maps³ (N=96) were randomly extracted from an anonymized data repository of NAFLD clinical trials (c.f. Fig. 1).

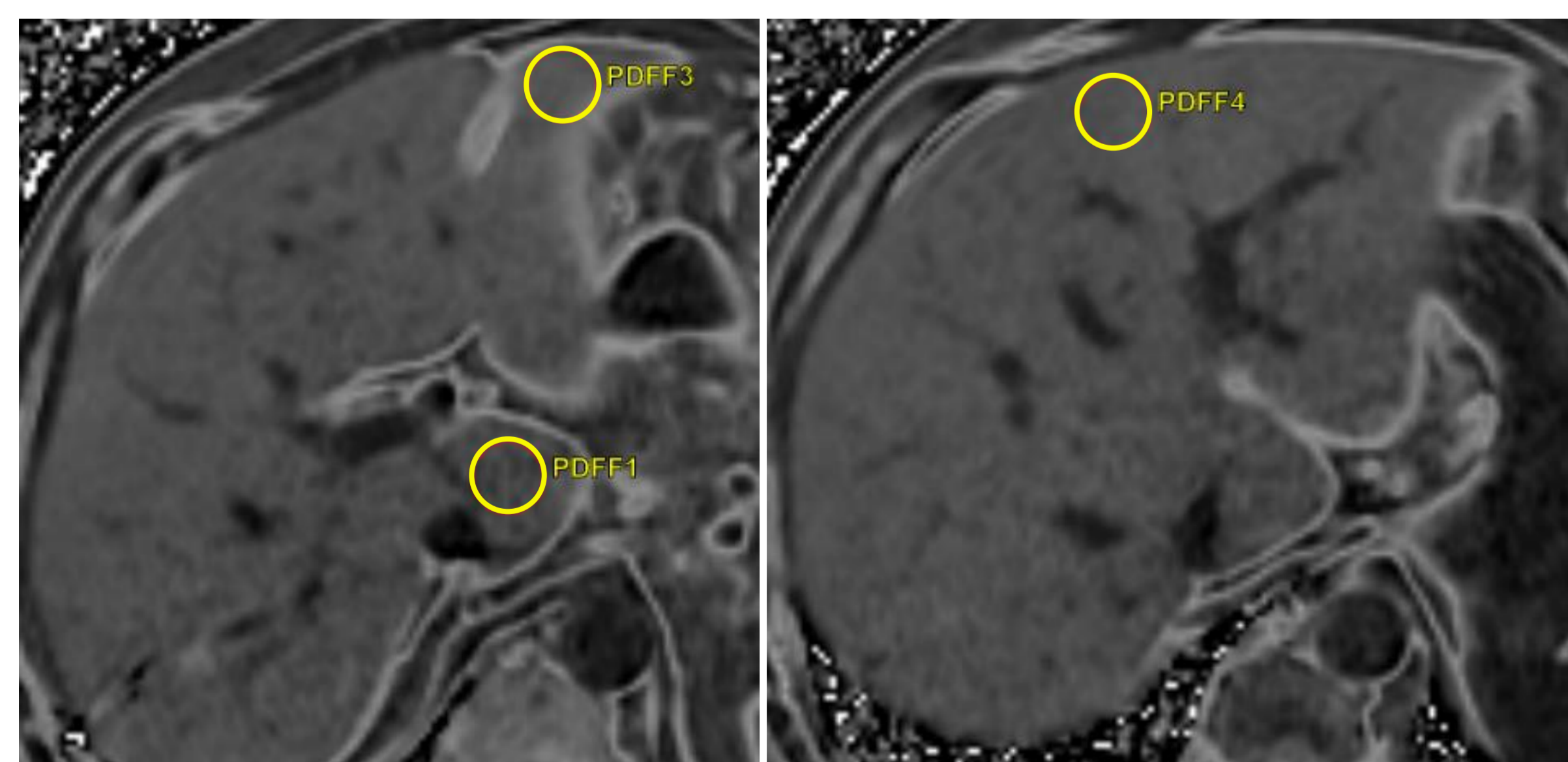


Fig. 1: Example of PDFF maps with ROIs.

- ROIs were placed in each of 9 Couinaud segments^{2,4} (c.f. Fig. 2 left).
- aPDFF was calculated over the complete set of 9 ROIs and over all combinations of 1 to 8 ROIs⁵.

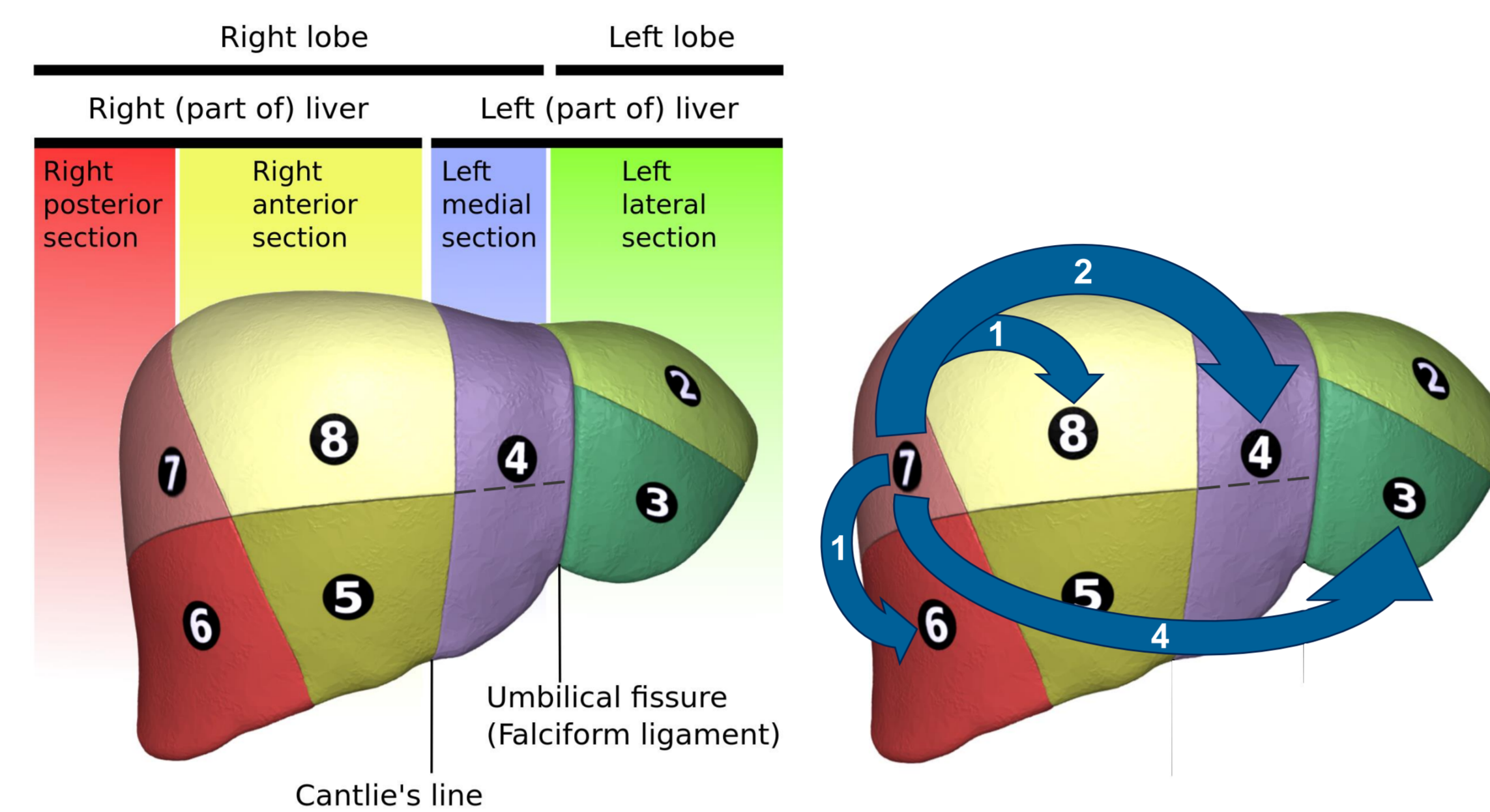


Fig. 2: (left) Liver segment classification by Couinaud⁷ (S4 is split into S4a and S4b, S1 is posterior to S4) (right) Inter-segment distances used for dispersion score calculation.

- A “Dispersion” score was calculated for each combination of ROIs:
 - It reflects the spatial distribution of the ROIs in the liver.
 - The higher the score, the higher the average distance between the ROIs.
 - It is based on a simple inter-segment distance metric (c.f. Fig. 2 right) which is worth 1 for two contiguous segments (e.g. S6 and S7 or S8 and S5) and reaches a maximum value 4 for the most distant pairs (e.g. S7 and S3 or S6 and S2).
- ROI combinations were split in two groups for analysis:
 - “High”: Quartile of ROI combinations with highest dispersion score (e.g. 3 ROIs in S2, S4b and S8 which has a dispersion score of 3).
 - “Low”: Other three quartiles (e.g. 3 ROIs in S6, S7 and S8 which has a dispersion score of 1.33).
- aPDFF for each ROIs combination was compared to the aPDFF from 9 ROIs using the following statistical measures:
 - Intraclass Correlation Coefficient (ICC).
 - Absolute Error (AE) in aPDFF expressed in % point.
 - 95% Limits Of Agreement⁶ (LOA).

4 RESULTS

- High dispersion performs better than Low for all 3 metrics (c.f. Table 1).

	Disp.	N	ICC (μ)	ICC (σ)	LOA (μ)	LOA (σ)	AE (μ)	AE (σ)
2 ROIs	High	8	0.990	1.10⁻³	2.85	0.251	0.881	0.053
	Low	26	0.985	6.10 ⁻³	3.59	0.613	1.06	0.198
3 ROIs	High	16	0.994	1.10⁻³	2.30	0.232	0.696	0.082
	Low	68	0.991	3.10 ⁻³	2.63	0.451	0.797	0.141
4 ROIs	High	19	0.996	1.10⁻³	1.85	0.235	0.551	0.080
	Low	107	0.995	2.10 ⁻³	2.05	0.350	0.629	0.107

Table 1: Summary of statistical measures for 2 to 4 ROIs combination grouped by dispersion (high/low). Other ROIs combination do not show statistical differences.

- Individual PDFF values are comparable across liver segments (c.f. Fig. 3).

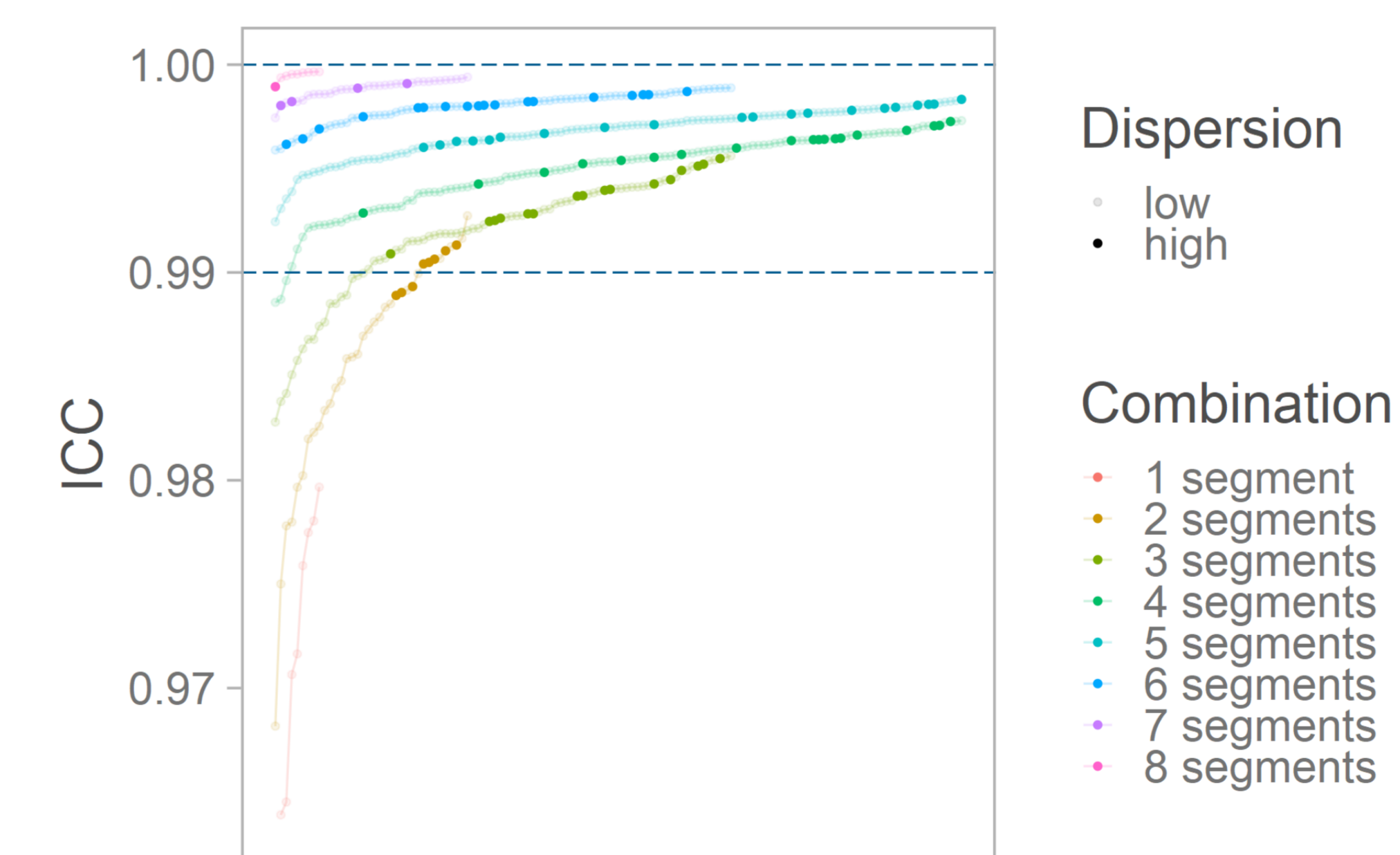


Fig. 4: ICC score per ROIs combination. Bold dots have the 25% higher dispersion in the combination of ROIs.

- ROI combinations with higher dispersion score result in higher and stable values of ICC, AE and LOA metrics (c.f. Fig. 4 and Table 1, High dispersion ROIs are bold in Fig. 4).
- aPDFF from more ROIs leads to increased correlation with 9 ROIs for ICC, AE and LOA metrics (c.f. Fig. 4).

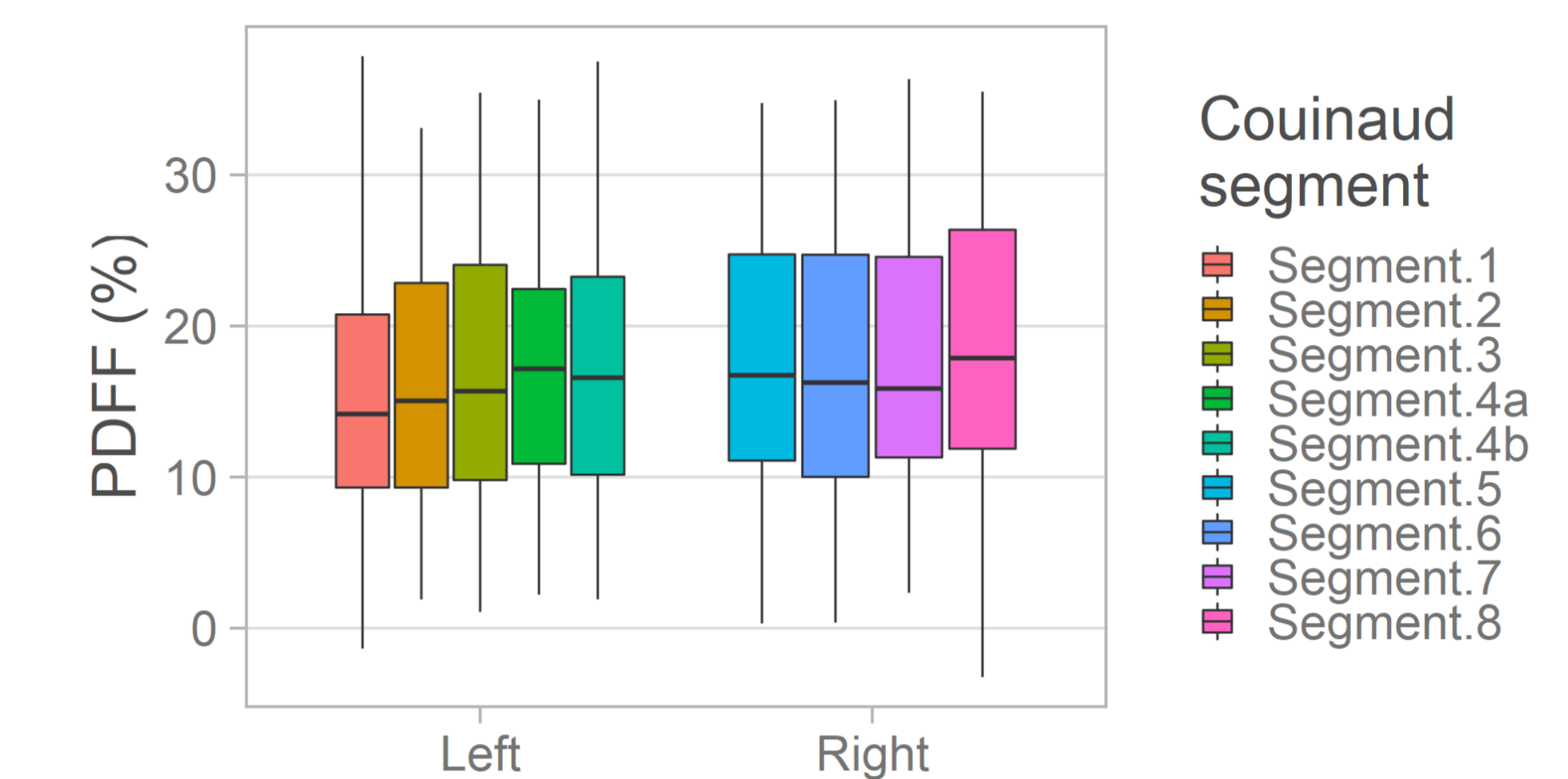


Fig. 3: Overview of PDFF values per Couinaud segments (N=96).

5 CONCLUSIONS

- aPDFF over fewer ROIs with the greatest dispersion produces a valid and reliable alternative to using 9 ROIs.
- Fewer ROIs can be placed more efficiently and reliably across the liver (avoiding vessels or artifacts).
- 3 ROIs selected with High dispersion (e.g. S2, S4b and S6) yield >99% agreement with aPDFF calculated over 9 ROIs covering all Couinaud segments of liver.

6 REFERENCES

1. Yokoo T, et al. Linearity, Bias, and Precision of Hepatic Proton Density Fat Fraction Measurements by Using MR Imaging: A Meta-Analysis. Radiology. 2018;286:486-98.
2. Couinaud C. Erreur dans le diagnostic topographique des lésions hépatiques. Ann Chir. 2002;127:418-30.
3. Zhong X, et al. Liver fat quantification using a multi-step adaptive fitting approach with multi-echo GRE imaging. Magn Reson Med. 2014;72:1353-65.
4. Germain T, et al. Liver segmentation: practical tips. Diagn Interv Imaging. 2014;95:1003-16.
5. Hong CW, et al. Optimization of region-of-interest sampling strategies for hepatic MRI proton density fat fraction quantification. J Magn Reson Imaging. 2018;47:988-94.
6. D. Giavarania. Understanding Bland Altman analysis. Biochemia Medica 2015;25(2):141-51
7. Database Center for Life Science (DBCLS). Polygon data is from BodyParts3D (CC BY-SA 2.1 jp) <https://commons.wikimedia.org/w/index.php?curid=45604146>

7 CONTACT

Tel: +33 4 37 53 09 80 (ext. 25455)
E-mail: f.roche@medpace.com
www.medpace.com